J Surfact Deterg (2018) **21:** 433–440
DOI 10.1002/jsde.12036

ORIGINAL ARTICLE

Aggregation-Enhanced Emission of Fluorescent-Gemini Surfactants with High Photostability for Cell-Membrane Imaging

Jinwen Peng[1] · Junjie Deng[1] · Xuebing Huang[1] · Pengfei Sun[2] · Weixing Deng[1]

Received: 5 May 2017 / Revised: 5 October 2017 / Accepted: 20 December 2017

Abstract *In situ* studies of the aggregation behavior of traditional surfactants at the liquid interface using spectroscopic methods are often significantly affected by the large volume of fluorescent groups, such as pyrene. Fluorescent-Gemini surfactants provide an ideal solution since the fluorescent block can be designed as a spacer or a tail. In this work, we report the synthesis of a new fluorescent-Gemini surfactant with a rigid spacer (referred to as 8-TBT-8). The aggregation behavior and application in cell-membrane imaging were investigated. The unique aggregation behavior in an organic solvent and aqueous solution was studied using spectroscopy. UV–vis and photoluminescence spectra of 8-TBT-8 revealed that this new fluorescent surfactant forms H aggregates in organic solution to give blue emission, whereas it forms J aggregates in aqueous solution to give green fluorescence under UV light. In addition, the fluorescence intensity of 8-TBT-8 increases abruptly at concentrations higher than the critical micellization concentration. Good photostability and a unique structure make the synthesized Gemini surfactant very suitable for membrane imaging.

Electronic supplementary material The online version of this article (doi:10.1002/jsde.12036) contains supplementary material, which is available to authorized users.

✉ Weixing Deng
freewxdeng@163.com; wxdeng@glut.edu.cn

[1] Guangxi Ministry-Province Jointly-Constructed Cultivation Base for State Key Laboratory of Processing for Non-Ferrous Metal and Featured Materials, Guilin University of Technology, Guilin, 541004, China

[2] Key Laboratory for Organic Electronics & Information Displays, Institute of Advanced Materials, Nanjing University of Posts & Telecommunications, Nanjing, 210046, China

Keywords Gemini surfactant · Aggregation-enhanced emission · Fluorescent surfactant · Cell imaging

J Surfact Deterg (2018) **21:** 433–440.

Introduction

Gemini surfactants have been attracting extensive interest due to their unique self-assembly behavior both at interfaces and in solutions (Zana, 2002). Much attention has been devoted to studies of their synthesis methods, hierarchal structures, and applications in various fields, including sensors (Hong et al., 2013), drug vectors (Giuliani et al., 2015), gene delivery (Fisicaro et al., 2014), DNA transfection (Zhou et al., 2013), membranes (Nieves et al., 2015), and antibacterial agents (Zhang et al., 2015). So far, different Gemini surfactants, including quaternary ammonium, anionic, nonionic, and zwitterionic, have been designed and synthesized. Furthermore, the solution behavior and properties of Gemini surfactants have been well illustrated. However, few fluorescent-Gemini surfactants have been reported, and accordingly related phenomena are not yet well understood (Nieves et al., 2015; Takahashi, Fukuyasu, Horiuchi, Kondo, & Stroeve, 2013; Zhang et al., 2015).

Fluorescent blocks are functional emissive units and have found applications in solar cells (Cheng, Yang, & Hsu, 2009), organic light-emitting diodes (Grimsdale, Leok, Martin, Jokisz, & Holmes, 2009), and probes (Chen & Yin, 2014; Zhu, Liu, Yang, Lv, & Wang, 2012). By introducing fluorescent blocks into surfactants, it is possible to investigate the aggregation behavior of surfactants using spectral analysis. Compared with traditional methods, such as surface tensiometry (Zhang et al., 2014),

conductimetry (Łudzik, Kustrzepa, & Piekarski, 2014; Łudzik, Kustrzepa, Piekarski, & Jóźwiak, 2016), rheology (Lu, Huang, Li, Jia, & Fu, 2008), isothermal-titration calorimetry (Li, Wettig, & Verrall, 2004), and dynamic-light scattering (Cuenca, Falcone, Silber, & Correa, 2016), spectroscopy shows advantages. In fact, pyrene has been used to study micellar systems for a long time due to its sensitivity to microenvironments (Kalyanasundaram & Thomas, 1977). Based on the spectral properties of pyrene, Ge et al. (2012) studied the assembly of anionic-Gemini surfactants in the presence of bovine serum albumin. Wang, Wettig, Foldvari, and Verrall (2007) introduced a 1-pyrenehexyl unit as one of the hydrophobic tails to yield a pyrene-substituted Gemini surfactant. Keyes-Baig, Duhamel, and Wettig (2011) used time-resolved fluorescence to characterize the behavior of pyrene-substituted Gemini surfactants in solution. Though plausible, the large volume of the pyrene does affect the assembly behavior of these surfactants. In fact, except hydrophobic tails, spacer linkers in Gemini surfactants that can be designed as fluorescent units also have many varieties. Conjugated units including fluorene, thiophene, carbazole, and pyrrole also deserve to be exploited.

It is of great importance for cell-membrane imaging to analyze the cell morphology, and the structure of cellular membranes often folds into various shapes with different morphologies to perform a variety of functions (McMahon & Gallop, 2005; Shibata, Hu, Kozlov, & Rapoport, 2009). Fluorescent probes have been used to monitor biological processes both in membrane models and in cellular experiments with high-temporal and spatial resolution (Shim et al., 2012). Cell-membrane probes are supposed to mimic the structure and behavior of natural lipids. Nieves et al. (2015) developed three ceramide analogs containing five conjugated double bonds as membrane probes to study sphingolipids in membranes. The stability of fluorophores *in vivo* is another important consideration since most traditional fluorophores suffer due to photobleaching. For high-bright photoluminescence (PL) and photostability, Zhang et al. (2012) prepared carboxylic-acid-modified semiconducting polymer nanoparticles using the coprecipitation method to label human breast cancer cells. Li et al. (2014) developed conjugated-polymer nanoparticles functionalized with plerixafor using a miniemulsion method for cell-membrane imaging. Gemini surfactants have a similar structure to phospholipids making them suitable for cell imaging. Because the emission spectra are sensitive to the aggregation of these Gemini-surfactant molecules, fluorescent-Gemini surfactants promise access to the imaging of not only the lateral organization of biomembranes but also membrane potentials, poorly detectable membrane tension, and so on. However, these functions are beyond the reach of traditional dyes for imaging methods. To our knowledge, fluorescent-Gemini surfactants with a conjugated unit as a spacer have not been used in cell-membrane imaging.

In this work, we first present a fluorescent-Gemini surfactant with aggregation-enhanced emission to label live-cell membranes. This quaternary-ammonium probe (8-TBT-8) comprises a thiophene–benzene–thiophene chromophore and two alkane tails. 8-TBT-8 favors the formation of H aggregates in an organic solvent to give blue emission, whereas it forms J aggregates in an aqueous medium to give green fluorescence under UV light. Spectroscopy measurements reveal that the fluorescent surfactant 8-TBT-8 aggregates in micelles at 1×10^{-6} mol L^{-1} and these micelles show high photostability, which is suitable for membrane imaging.

Experimental Procedures

Materials

2,5-Dibromohydroquinone, 2-chloroethyldiethylamine, 2-(tributylstannyl)thiophene, octanoyl chloride, bromomethane, and stannic chloride were purchased from Sigma–Aldrich (Louis, USA) and used without further purification. Tetrahydrofuran (THF) and CCl_4 were dried over sodium benzophenone ketyl and distilled under a dry nitrogen atmosphere immediately prior to use. Dulbecco's modified Eagle's medium (DMEM, Gibco, USA) was purchased from Gene Tech Co. (Shanghai, China). Spectrochemical-grade solvents were used for optical measurements.

General Method

Nuclear magnetic resonance (NMR) spectra were recorded on a Bruker 400 MHz spectrometer (Billerica, MA, USA) in $CDCl_3$ or dimethyl sulfoxide-d_6 with tetramethylsilane as the internal standard. Absorption spectra were measured using a Shimadzu UV-3150 spectrometer (Kyoto, Japan) at 25 °C, and PL spectra were recorded on a Shimadzu RF-530XPC luminescence spectrometer upon excitation at the absorption maxima. Dynamic light scattering (DLS) measurements were carried out using a Brookhaven Instruments Corporation 90 Plus instrument (NY, USA) with $\lambda = 532$ nm and scattering angles are 90°. Hydrodynamic diameters were calculated using the nonnegative least-squares method. Zeta potentials were measured using a zeta potential analyzer (Zeta PALS, Brookhaven Instruments Corp). Fluorescence images were obtained with a confocal laser scanning microscope (TCS SP5, Leica, Mannheim, Germany). The photostability of fluorescent-Gemini surfactant micelles was investigated using an Edinburgh FLSP920 fluorescence spectrophotometer (Edinburgh, UK).

Cell Imaging

The cells were first cultured in confocal microscopy dishes at an intensity of 4×10^4 cm^{-2} in a complete DMEM medium and cultured for 24 h at 37 °C. Then, the cells were washed with phosphate buffer saline (PBS) and treated with a medium containing 8-TBT-8 (10^{-6} M). After incubation for 10 min at 37 °C, the cells were rinsed twice with PBS and the cellular uptake of 8-TBT-8 was visualized using a confocal laser scanning microscope.

Synthesis of 1,4-Dibromo-2,5-bis(diethylaminoethoxy) Benzene (1)

A mixture of 2,5-dibromohydroquine (27 g, 0.1 mol), 2-diethylaminoethyl chloride hydrochloride (41 g, 0.3 mol), potassium carbonate (82 g, 0.6 mol), and anhydrous acetone 300 mL was stirred at 65 °C for 10 h. Then, it was cooled to room temperature and water was added. The product was extracted with dichloromethane (DCM). The combined organic layers were washed with aqueous solution of $NaHCO_3$ and dried over $MgSO_4$. In the next step, the solvent was evaporated under reduced pressure. The resulting crude products were purified by column chromatography (silica gel, EtOAc/petroleum ether with 1% triethylamine, 1:10). Yield: 86%. ^{1}H NMR (400 MHz, $CDCl_3$): δ 7.12 (2H), 4.02 (4H), 2.91 (4H), 2.64 (4H), 1.07 (12H) (Fig. S1). Matrix assisted laser desorption/Ionization time of flight mass spectrometry (MALDI-TOF-MS) (*m/z*) calcd for $C_{18}H_{30}Br_2N_2O_2$ $[M]^+$: 466.07, found: 465.46 (Fig. S2).

Synthesis of 1,4-Bis(thiophen-2-yl)-2,5-bis (diethylaminoethoxy) Benzene (2)

The target compound **2** was obtained *via* Stille reactions between 1 and 2-(tributylstannyl)thiophene in the presence of a catalytic amount of $Pd(PPh_3)_2Cl_2$. In an oven-dried round-bottom flask, 1,4-dibromo-2,5-bis(diethylaminoethoxy) benzene (2.23 g, 4.5 mmol) and 2-(tributylstannyl)thiophene (8 mL, 25 mmol) were dissolved in 40 mL anhydrous 1,4-dione. Bis(triphenylphosphine)palladium dichloride (0.31 g, 0.44 mmol) was added quickly. After degassing for 30 min, the mixture was stirred at 90 °C for 48 h under a nitrogen atmosphere. The solvent was evaporated under vacuum. The residue was dissolved in a mixture of DCM (200 mL), and the resulting solution was washed with statured Potassium fluoride (KF) solution (100 mL), water, and brine, respectively, and dried over anhydrous $MgSO_4$. The crude product was purified by column chromatography (silica gel, EtOAc/petroleum ether with 1% triethylamine, 1:10). Yield: 72%. ^{1}H NMR (400 MHz, $CDCl_3$): δ 7.56 (2H), 7.34 (2H), 7.29 (2H), 7.11 (2H), 4.16 (4H), 2.99 (4H), 2.64 (4H), 1.08 (12H) (Fig. S3). MALDI-TOF-MS (*m/z*) calcd for $C_{26}H_{36}N_2O_2S_2$ $[M]^+$: 472.22, found: 471.35 (Fig. S4).

Synthesis of P and 8-TBT-8

As shown in Scheme 1, compound P was prepared *via* the Friedel–Crafts reaction, $SnCl_4$ (1 mL, 8 mmol) was first added to a cold solution containing 1,4-bis(thiophen-2-yl)-

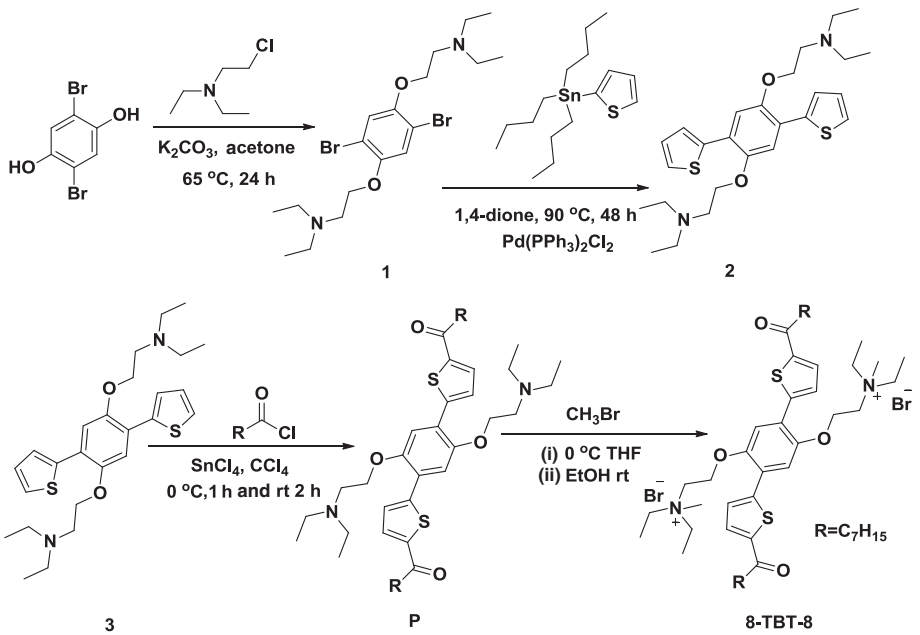

Scheme 1 Synthesis route to fluorescent-Gemini surfactants

2,5-bis(diethylaminoethoxy) benzene (2.36 g, 5 mmol), and then octanoyl chloride (3.4 mL, 20 mmol) in 8 mL CCl_4 was added with vigorous stirring. The reaction mixture was stirred for 1 h in an ice bath and allowed for additional 2 h reaction at room temperature. Then, 3 mL 2 M HCl was added slowly. The product was extracted with DCM. The organic layer was washed with aqueous $NaHCO_3$ and water then dried with $MgSO_4$. The solvent was removed with a vacuum evaporator and the product was purified by chromatography (silica gel, EtOAc/petroleum ether with 1% triethylamine, 1:10). Yield: 40%. Fluorescent-Gemini surfactant (8-TBT-8) was synthesized by reacting P with bromomethane in THF at 0 °C for 4 h. Water was then added and kept stirring for 12 h at room temperature. 8-TBT-8 was obtained as a yellow powder by freeze-drying. Detailed ^{1}H NMR spectra of P and 8-TBT-8 are shown in Fig. 1.

Results and Discussion

Synthesis and Molecular Characterization

The target compound was prepared starting from 2,5-dibromohydroquinone, which reacts with 2-chloroethyldiethylamine to give 1,4-dibromo-2,5-bis(diethylaminoethoxy) benzene (**1**) in 86% yield. 1,4-Dibromo-2,5-bis(diethylaminoethoxy) benzene was converted to 1,4-bis(thiophen-2-yl)-2,5-bis (diethylaminoethoxy) benzene (**2**) by the Stille coupling reaction with 2-(tributylstannyl)thiophene for 48 h in the presence of a catalytic amount of $Pd(PPh_3)_2Cl_2$ with the yield of 72%. Subsequently, compound P was prepared *via* the Friedel–Crafts reaction with octanoyl chloride in the yield of 40%. Finally, the cationic fluorescent-Gemini surfactant (8-TBT-8) was obtained by further treating compound P with bromomethane in THF with 85% yield.

All the compounds were confirmed using ^{1}H NMR. As compared to compound P, two new peaks at 3.81 and 3.06 ppm appear in the ^{1}H NMR of 8-TBT-8, which were assigned to N^+—CH_2 and N^+—CH_2—CH_3, respectively, while the peak at 3.01 ppm assigned to —OCH_2—CH_2—N— disappears; we think that it is overlapped by the trace H_2O signal in d-DMSO. Due to the amphiphilicity of the Gemini surfactant, it is difficult to obtain a clear ^{1}H NMR spectrum in other deuterated solvents.

Optical Properties

Figure 2 shows the UV–vis spectra and PL spectra of 8-TBT-8 (10^{-5} mol L^{-1} in units of rod block) in DCM and

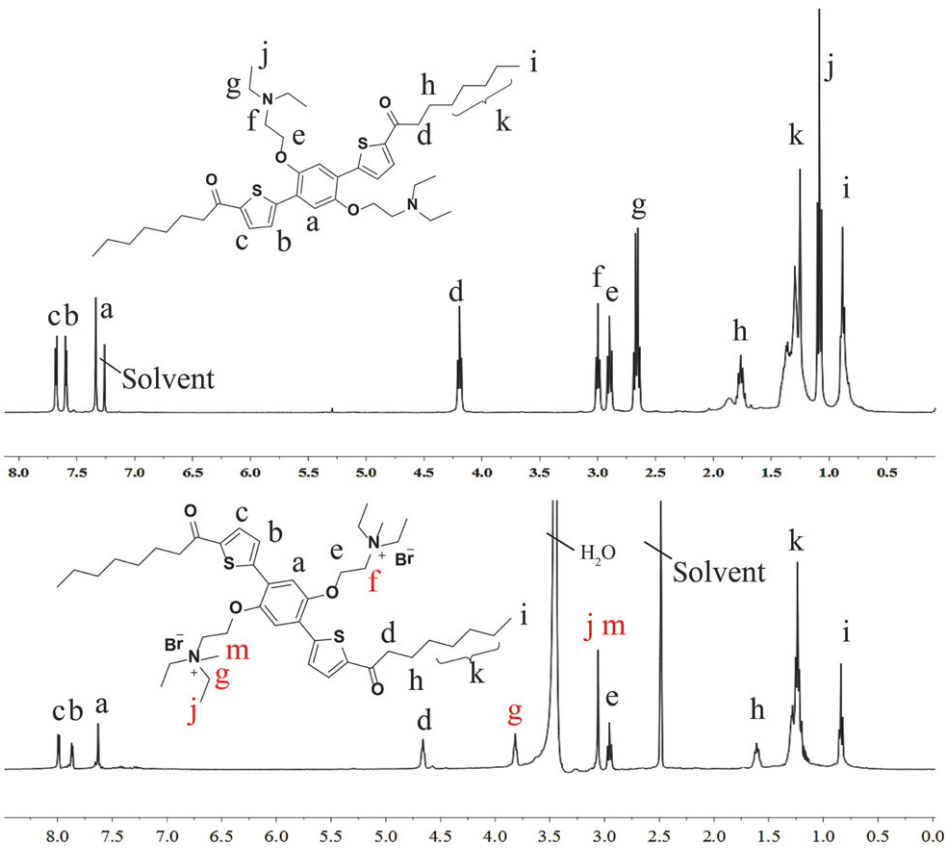

Fig. 1 ^{1}H NMR spectra of compound P in $CDCl_3$ (up) and 8-TBT-8 in DMSO-d_6 (down)

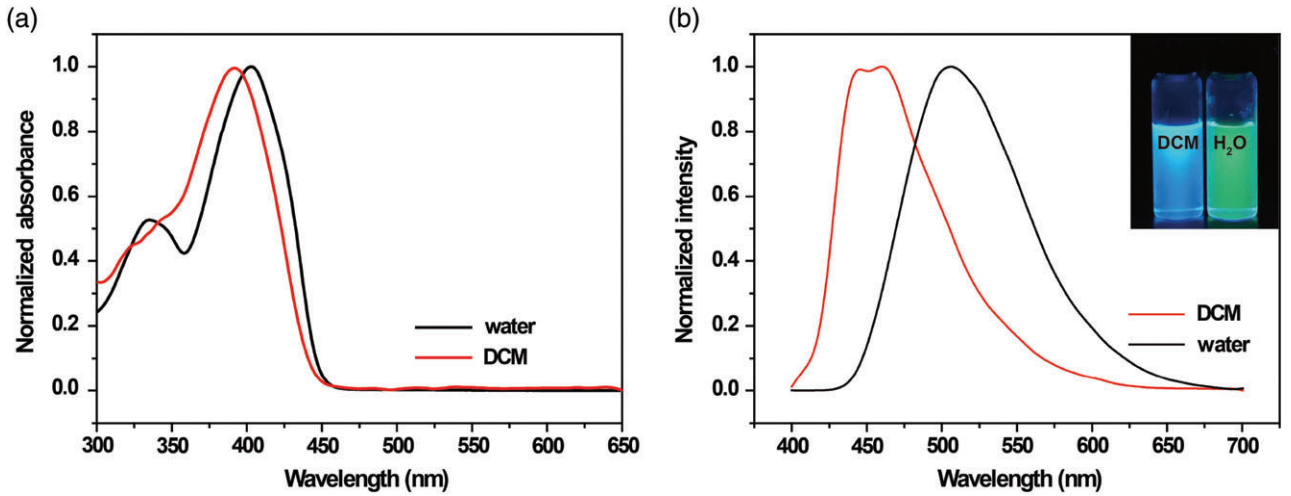

Fig. 2 UV–vis spectra (a) and PL spectra (b) of 8-TBT-8 in different solvents. The inset shows fluorescent colors of 8-TBT-8 in DCM and aqueous solution

aqueous solution. 8-TBT-8 has maximum absorption peaks at 391 nm in DCM and 402 nm in aqueous solution, which are attributed to π–π* transition intramolecular charge-transfer between benzene rings and thiophene rings. In addition, 8-TBT-8 shows a shoulder absorption peak at 334 nm in aqueous solution, which is assigned to the effect of carbonyl groups in the 8-TBT-8 unit. A similar bathochromic shift takes place in the emission spectra of the Gemini surfactant (8-TBT-8) and reveals solvent-dependent fluorescence emission. 8-TBT-8 shows two emission peaks at 445 and 459 nm in DCM and a single band at 505 nm in aqueous solution; this solvent-dependent change can be distinguished by the naked eye under UV light (Fig. 2, inset). It is obvious that the optical properties of 8-TBT-8 in DCM are different from the optical properties of compound P in DCM (Figs. S5 and S6). Compounds P and 8-TBT-8 share the same conjugated block but show different optical properties in the same solvent indicating that the conjugated blocks take different aggregation. The optical properties illustrate the aggregation behavior of 8-TBT-8 in DCM and aqueous solution (Figs. S7–S11 and 5a). In aqueous solution, the variation of the aggregation of 8-TBT-8 molecules was further improved due to the amphiphilicity of 8-TBT-8.

Compared with the emission spectra of 8-TBT-8 in DCM, the blue-shifted emission in aqueous solution is attributed to the assembly of a H-aggregate structure, in which dyes tend to form a head-to-tail or head-to-head aggregates of the rod units (Fig. 3a). On the other hand, the J-aggregated structure is attributed to parallel packing of rod units exhibiting a red-shift in the emission spectra (Fig. 3b). The long rigid spacer and two alkyl tails make 8-TBT-8 soluble in an organic solvent and these rigid spacers favor H-type aggregates through π–π stacking interactions. In DCM solution, the rod unit has good solubility and undergoes head-to-head aggregation. However, in aqueous solution, alkane chains with charges have better solubility than rod units and rod units form J-type aggregates through the hydrophobic interactions and electrostatic repulsion. This red-shifted emission of 8-TBT-8 in aqueous solution is beneficial for cell imaging.

The self-assembly behavior of 8-TBT-8 in aqueous solution was investigated by DLS. Figure 4 shows the hydrodynamic radius distribution of 8-TBT-8 in aqueous solution with the mean diameter of 182 nm at a concentration of 10^{-5} mol L^{-1}. Zeta potential of the 8-TBT-8 Gemini surfactant is 45 mV in aqueous solution. The particle size of 8-TBT-8 molecules in aqueous solution far outweighs the size of a single molecule of 8-TBT-8 indicating the aggregation of 8-TBT-8 molecules in aqueous solution. The high value of zeta potential enables a highly positive charge density on the surface of aggregated particles.

To study the aggregation behavior of the Gemini surfactant (8-TBT-8) in aqueous solution, the critical micelle concentration (CMC) was determined by the fluorescence intensity change *versus* the 8-TBT-8 concentration curve. Due to the hydrophobicity of the thiophene–benzene–thiophene unit, 8-TBT-8 yields very weak emission signals when the concentration is lower than the CMC. However, the fluorescence intensity increases significantly when 8-TBT-8 aggregates into micelles, which provide a relatively hydrophobic microenvironment for the thiophene–benzene–thiophene units (Fig. S11). The CMC of the Gemini surfactant (8-TBT-8) is 1×10^{-6} mol L^{-1} determined from the breakpoint of the fluorescence intensity as shown in Fig. 5. Such a low CMC value is mainly because the dimer structure of 8-TBT-8 has two hydrophobic alkyl chains rather than one. Figure 5 also shows the photostability of

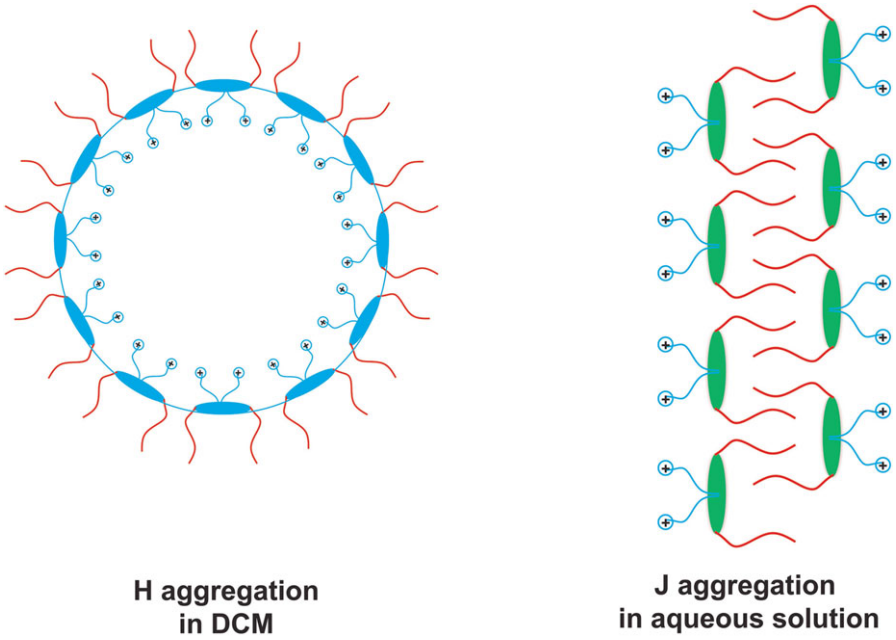

Fig. 3 H aggregates and J aggregates of 8-TBT-8 in DCM and aqueous solution

8-TBT-8 micelles both in DCM and in aqueous solution. The PL intensity remains almost unchanged after 10 min of continuous UV irradiation. These results reveal that 8-TBT-8 micelles are highly resistant to photobleaching and exhibit excellent photostability.

Cell Viability and Cell Uptake

Gemini surfactants have a similar structure to phospholipids with two hydrophobic alkane tails and hydrophilic cationic head groups, so they may aggregate on cell membranes just like phospholipids. Cytotoxicity of 8-TBT-8 was evaluated in a 3-(4, 5-dimethylthiazol-2-yl)-2, 5-diphenyltetrazolium bromide (MTT) cell viability assay against NIH-3T3 and it shows low cytotoxicity at low concentrations (Fig. S12). The cell imaging assay of 8-TBT-8 was performed for HeLa and HepG2 cells (Fig. 6). As expected, confocal laser scanning microscopy imaging results show that 8-TBT-8 is located on the membrane after 10 min incubation, which was verified by colocalization with a cell-membrane dye Dil. These cells show green channel and red channel fluorescence, respectively. The merged images indicate that the staining of 8-TBT-8 fits well with the cell-membrane dye Dil. The intensity channel also varies in close synchrony. Moreover, the intensity scatter plot of the green channel and the red

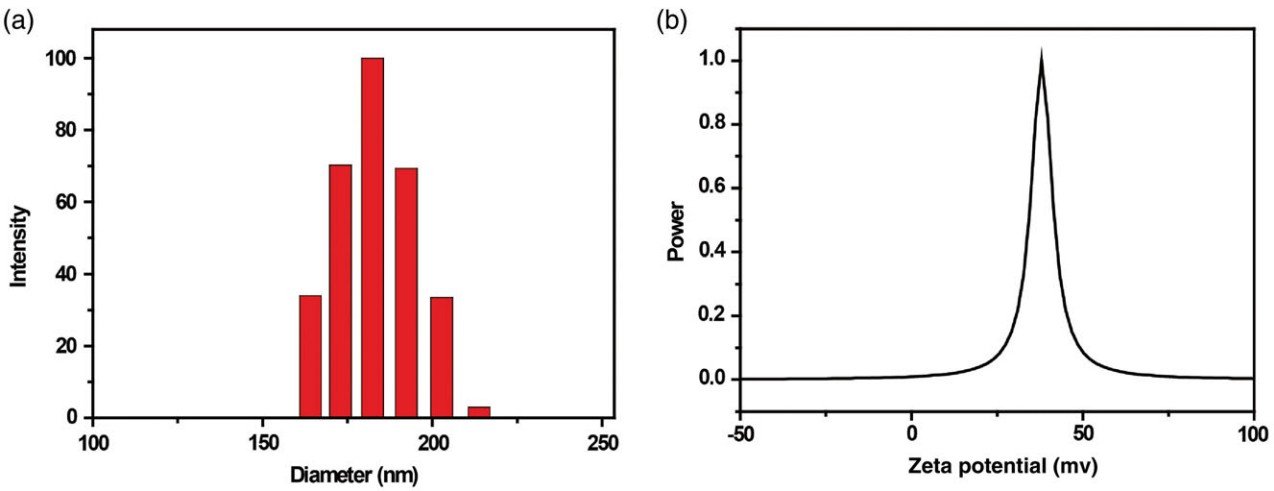

Fig. 4 Hydrodynamic size distribution (a) and zeta potential (b) of 8-TBT-8 in water

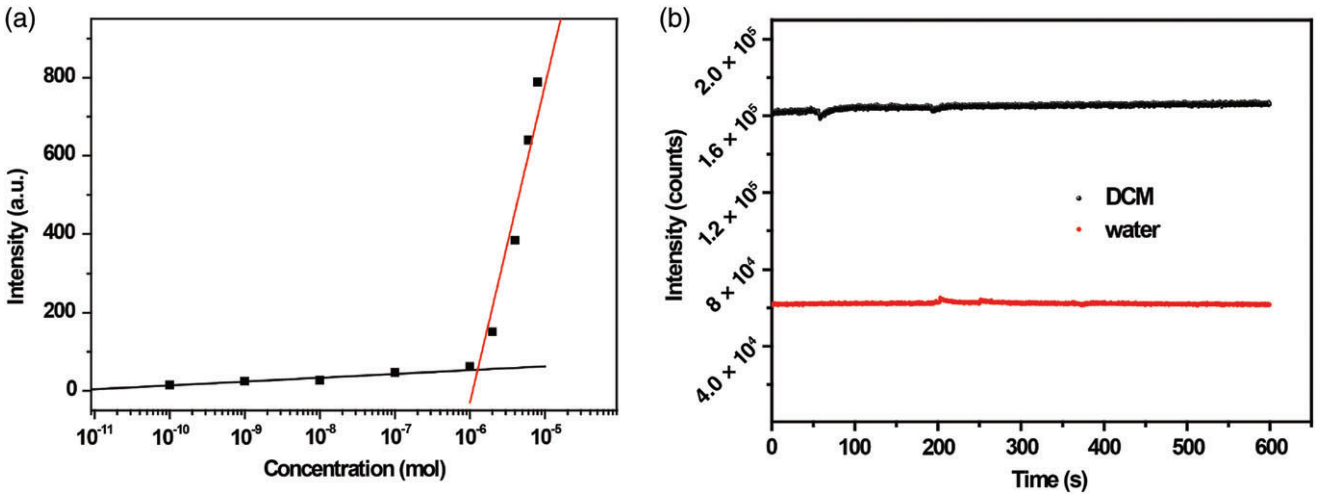

Fig. 5 Plot of fluorescence intensity for 8-TBT-8 (λex = 402 nm) *versus* log[8-TBT-8] (a) and luminescence time traces of 8-TBT-8 under UV light illumination for 10 min (b), indicating the high photostability of 8-TBT-8 in both DCM and aqueous solution

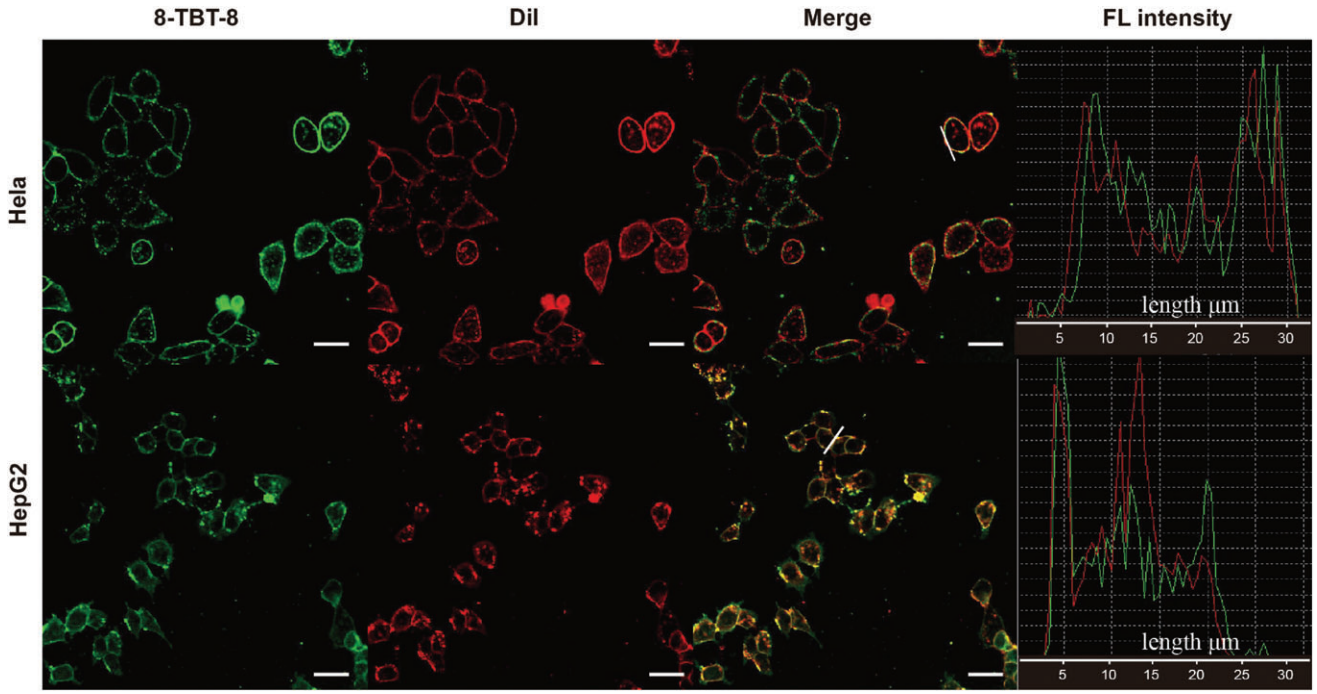

Fig. 6 Confocal luminescence images and intensity profiles across cells costained by 8-TBT-8 and DiI. Scale bar represents 30 μm

channel is highly correlated with a high-overlap Pearson's coefficient (0.86 for HeLa cells and 0.92 for HepG2 cells). The results further confirm that fluorescent-Gemini surfactant (8-TBT-8) mainly locates in the cell membrane.

Conclusions

A fluorescent-Gemini surfactant (8-TBT-8) with a thiophene–benzene–thiophene-conjugated spacer was synthesized and its spectral properties were investigated. It was found that 8-TBT-8 forms H aggregates to give a blue emission and forms J aggregates to give a green fluorescence upon UV irradiation. Spectrometry showed that the fluorescent surfactant 8-TBT-8 aggregates into micelles at 1×10^{-6} mol L^{-1}, the micelles formed have high photostability, which is suitable for membrane imaging. Water soluble 8-TBT-8 showed low cytotoxicity at low concentrations and located on cell membranes effectively.

Acknowledgements This work was financially supported by the National Natural Science Foundation of China (No. 51363004), Natural Science Foundation of Guangxi (2014GXNSFBA118244), Guangxi Universities Science Research Project (YB2014154), and Key

Laboratory of New Processing Technology for Nonferrous Metals and Materials (13KF-2).

References

Chen, M. J., & Yin, M. Z. (2014) Design and development of fluorescent nanostructures for bioimaging. *Progress in Polymer Science*, **39**:365–395.

Cheng, Y.-J., Yang, S.-H., & Hsu, C.-S. (2009) Synthesis of conjugated polymers for organic solar cell applications. *Chemical Reviews*, **109**:5868–5923.

Cuenca, V. E., Falcone, R. D., Silber, J. J., & Correa, N. M. (2016) How the type of cosurfactant impacts strongly on the size and interfacial composition in Gemini 12-2-12 RMs explored by DLS, SLS, and FTIR techniques. *Journal of Physical Chemistry B*, **120**: 467–476.

Fisicaro, E., Compari, C., Bacciottini, F., Contardi, L., Barbero, N., Viscardi, G., … Sansone, F. (2014) Nonviral gene delivery: Gemini bispyridinium surfactant-based DNA nanoparticles. *Journal of Physical Chemistry B*, **118**:13183–13191.

Ge, Y. S., Tai, S. X., Xu, Z. Q., Lai, L., Tian, F. F., Li, D. W., … Gao, Z. N. (2012) Synthesis of three novel anionic Gemini surfactants and comparative studies of their assemble behavior in the presence of bovine serum albumin. *Langmuir*, **28**:5913–5920.

Giuliani, C., Altieri, B., Bombelli, C., Galantini, L., Mancini, G., & Stringaro, A. (2015) Remote loading of aloe emodin in Gemini-based cationic liposomes. *Langmuir*, **31**:76–82.

Grimsdale, A. C., Leok, C. K., Martin, R. E., Jokisz, P. G., & Holmes, A. B. (2009) Synthesis of light-emitting conjugated polymers for applications in electroluminescent devices. *Chemical Reviews*, **109**:897–1091.

Hong, W., Li, H. R., Hu, X. B., Zhao, B. Y., Zhang, F., Zhang, D., & Xu, Z. (2013) Wettability gradient colorimetric sensing by amphiphilic molecular response. *Chemical Communications*, **49**: 728–730.

Kalyanasundaram, K., & Thomas, J. K. (1977) Environmental effects on vibronic band intensities in pyrene monomer fluorescence and their application in studies of micellar systems. *Journal of the American Chemical Society*, **99**:2039–2044.

Keyes-Baig, C., Duhamel, J., & Wettig, S. (2011) Characterization of the behavior of a pyrene substituted Gemini surfactant in water by fluorescence. *Langmuir*, **27**:3361–3371.

Li, M., Nie, C. Y., Feng, L. H., Yuan, H. X., Liu, L. B., Lv, F. T., & Wang, S. (2014) Conjugated polymer nanoparticles for cell membrane imaging. *Chemistry—An Asian Journal*, **9**:3121–3124.

Li, X. F., Wettig, S. D., & Verrall, R. E. (2004) Interactions between 12-EOx-12 Gemini surfactants and pluronic ABA block copolymers (F108 and P103) studied by isothermal titration calorimetry. *Langmuir*, **20**:579–586.

Lu, T., Huang, J. B., Li, Z. H., Jia, S. K., & Fu, H. L. (2008) Effect of hydrotropic salt on the assembly transitions and rheological responses of cationic Gemini surfactant solutions. *Journal of Physical Chemistry B*, **112**:2909–2914.

Łudzik, K., Kustrzepa, K., & Piekarski, H. (2014) Thermodynamics of micelle formation of Gemini surfactants hexylene-1,6-bis (dimethyloctylammoniumbromide) and dodecylene-1,12-bis (dimethyloctylammonium bromide) by electric conductance measurements. *Journal of Chemical & Engineering Data*, **59**: 4165–4172.

Łudzik, K., Kustrzepa, K., Piekarski, H., & Jóźwiak, M. (2016) Application of conductance study to analyze micellization behavior of cationic Gemini surfactants in water and water–ethanol solvent mixed media. *Journal of Chemical & Engineering Data*, **61**: 1047–1053.

McMahon, H. T., & Gallop, J. L. (2005) Membrane curvature and mechanisms of dynamic cell membrane remodelling. *Nature*, **438**: 590–596.

Nieves, I., Artetxe, I., Abad, J. L., Alonso, A., Busto, J. V., Fajari, L., … Goni, F. M. (2015) Fluorescent polyene ceramide analogues as membrane probes. *Langmuir*, **31**:2484–2492.

Shibata, Y., Hu, J. J., Kozlov, M. M., & Rapoport, T. A. (2009) Mechanisms shaping the membranes of cellular organelles. *Annual Review of Cell and Developmental Biology*, **25**:329–354.

Shim, S.-H., Xia, C. L., Zhong, G. S., Babcock, H. P., Vaughan, J. C., Huang, B., … Zhuang, X. W. (2012) Super-resolution fluorescence imaging of organelles in live cells with photoswitchable membrane probes. *Proceedings of the National Academy of Sciences of the United States of America*, **109**:13978–13983.

Takahashi, Y., Fukuyasu, K., Horiuchi, T., Kondo, Y., & Stroeve, P. (2013) Photoinduced demulsification of emulsions using a photoresponsive Gemini surfactant. *Langmuir*, **30**:41–47.

Wang, C. Z., Wettig, S. D., Foldvari, M., & Verrall, R. E. (2007) Synthesis, characterization, and use of asymmetric pyrenyl-Gemini surfactants as emissive components in DNA-lipoplex systems. *Langmuir*, **23**:8995–9001.

Zana, R. (2002) Dimeric and oligomeric surfactants. Behavior at interfaces and in aqueous solution: A review. *Advances in Colloid and Interface Science*, **97**:205–253.

Zhang, S. S., Ding, S. P., Yu, J., Chen, X. R., Lei, Q. F., & Fang, W. J. (2015) Antibacterial activity, in vitro cytotoxicity, and cell cycle arrest of Gemini quaternary ammonium surfactants. *Langmuir*, **31**:12161–12169.

Zhang, S. S., Yu, J., Wu, J. Z., Tong, W., Lei, Q. F., & Fang, W. J. (2014) Micellization parameters of six Gemini quaternary ammonium surfactants from measurements of conductivity and surface tension. *Journal of Chemical & Engineering Data*, **59**:2891–2900.

Zhang, X. J., Yu, J. B., Wu, C. F., Jin, Y. H., Rong, Y., Ye, F. M., & Chiu, D. T. (2012) Importance of having low-density functional groups for generating high-performance semiconducting polymer dots. *ACS Nano*, **6**:5429–5439.

Zhou, T., Llizo, A., Li, P., Wang, C. X., Guo, Y. Y., Ao, M. Q., … Xu, G. Y. (2013) High transfection efficiency of homogeneous DNA nanoparticles induced by imidazolium Gemini surfactant as nonviral vector. *Journal of Physical Chemistry C*, **117**: 26573–26581.

Zhu, C. L., Liu, L. B., Yang, Q., Lv, F. T., & Wang, S. (2012) Water-soluble conjugated polymers for imaging, diagnosis, and therapy. *Chemical Reviews*, **112**:4687–4735.